

Studies of Resolution in a Bragg Imaging System

ROY A. SMITH,* GLEN WADE, JOHN POWERS, AND JOHN LANDRY

Department of Electrical Engineering, University of California, Santa Barbara, California 93106

This paper presents the results of experiment and theory concerning the resolution capabilities of a Bragg diffracting system which uses a cylindrically convergent laser beam for imaging objects which scatter sound. The derived theory predicts that thin wires, oriented parallel to the convergence line of the light beam and separated by one wire diameter, will just be resolved if the wire diameter is equal to $(\Lambda/2)/\sin\alpha_m$, where Λ is the sound wavelength and α_m is the semiangle of the light convergence. For wire orientation at right angles to this direction, the resolution is of quite a different character. The predicted wire diameter is then $(\Lambda/2)/\sin\theta_m$, where θ_m is half the angle subtending the light beam in the direction perpendicular to the wire axes. Copper wires as small as 10 sound wavelengths in diameter could be experimentally resolved in our system when the wires were oriented parallel to the convergence line of the light beam. When oriented at right angles, wires as small as $\frac{2}{3}$ of a sound wavelength could be resolved. These figures demonstrate good experimental verification of the theory.

INTRODUCTION

In 1922, Brillouin¹ predicted that a sound beam in a transparent medium could diffract plane waves of light. The critical angle for this diffraction was just that expressed by Bragg's formula for x-ray diffraction. In 1965, Cohen and Gordon² showed that the amplitude of the light thus diffracted, as a function of the angle of incidence of the input light, was proportional to the Fourier transform of the acoustic-amplitude distribution across the sound beam. The angular dependence of the diffracted light was therefore found to be a direct measure of the spatial distribution of the acoustic energy. In an extension of this principle, Korpel³ demonstrated that an arbitrary object, if irradiated with a planar ultrasonic wave, could be imaged optically. This was done by diffracting laser light from a line source with scattered sound. This technique is now known as Bragg imaging and has recently been used to exhibit internal structure in metallic and biological objects that are opaque to light but relatively transparent to sound.⁴

The image position in a conventional Bragg system is readily found by means of ray tracing. Assume that the object is a line source of sound (i.e., a line scatterer of the incident sound waves such as a thin straight wire) oriented in the same direction as the laser-line source. In this simple case, the light and sound rays all emerge perpendicular to their respective line sources.

If the line source is vertically oriented, all the light and sound rays are wholly contained in horizontal planes. The pattern of ray paths then has essentially a two-dimensional character and is easily traced on a sheet of paper representing one of the horizontal planes. The line sources then appear as intersection points on the paper. Each point represents a line that is assumed to extend perpendicularly through the paper. Image positions found in this fashion are precisely the kind that have previously been discussed in the literature.³

Recently, Korpel observed that for objects that give rise to sound rays scattered radially from a line normal to the light-source axis, the diffracted light rays produce an image located relatively far away from the image position discussed above.⁵ Thus two image locations can be found. Objects that are essentially line sources of sound (i.e., line scatterers) extending in the same direction as the line source of light will be imaged at one location. Assume the line source of light is vertically oriented. Objects that are essentially line sources of sound extending horizontally will be imaged at the other location.

Consider the case of line scatterers oriented horizontally. These will scatter sound radially. A ray-path diagram is not so easy to trace in this case because of the three-dimensional character of the diagram. However, if the rays are traced, it can be seen that the image focal point is in a different place for sound rays emerging from

this object with small vertical components than for sound rays emerging with large vertical components. The position of the focal point is a sensitive function of the angle of inclination of the scattered sound rays relative to the horizontal plane. Because of this fact, resolution for such an image might be expected to deteriorate, owing to aberrations if the sound rays used to produce the image are not restricted to those having small angles of inclination.

The purpose of this paper is to present the results of a number of experiments concerning the resolution capabilities of a Bragg imaging system. One of the experimental objectives was to measure the resolution for line scatterers oriented both vertically and horizontally. It was found that in the case of vertical orientation, the Rayleigh expression for resolution (assuming coherent illumination) is quite valid if the sine of the semiangle of the light wedge is used as the numerical aperture in the equation. For the case of horizontal orientation, the situation is substantially more complicated. An unexpected experimental result was the discovery that a small-angle restriction need not be imposed on the scattered sound rays. The aberrations were of a different character than first expected and did not substantially limit the resolution, even with angles approaching 90° . In our experiments the resolution was considerably better for horizontal orientation than for vertical orientation. Because of the mutually orthogonal character of the two types of images, it was relatively easy to design a system using two perpendicularly oriented cylindrical lenses that would bring together the two image locations onto the same image plane. Thus an object with horizontal and vertical scattering elements could be seen as a single integrated image with essential contributions coming from both image types.

I. DESCRIPTION OF SYSTEM

Figure 1 shows the system. An object to be viewed is placed in the acoustic cell located in the central region. The object is irradiated by sound (in water) generated by a quartz-plate transducer. Sound scattered by the object propagates to a region where coherent light

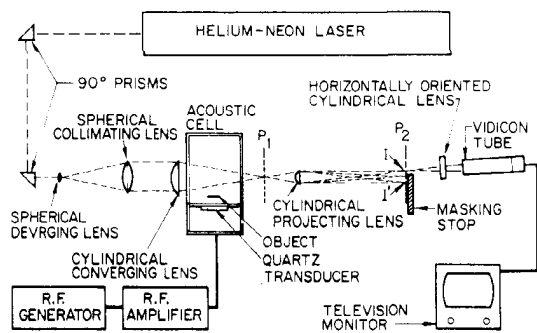


FIG. 1. Top view of the Bragg imaging system.

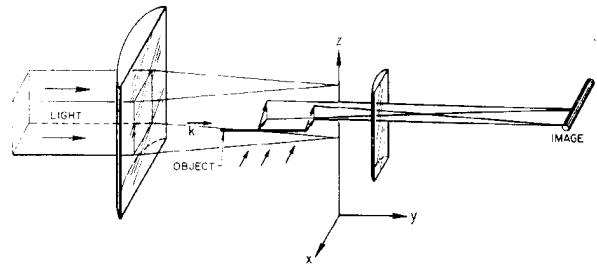


FIG. 2. Light and sound rays involved in imaging of a horizontal wire.

from a helium-neon laser is admitted into the cell. As shown in the figure, the object is located well outside this light field. Incident light rays are diffracted by the scattered sound. Diffraction occurs wherever the Bragg condition is satisfied. The laser light is formed into a cylindrically convergent wedge, and this allows the Bragg condition to be satisfied over a reasonably wide range of spatial frequencies. The down-converted sideband beam in the emerging light is brought to focus and forms a real image of the object.³ Note that for the case considered here, the zero-order and up-converted beams are blocked by a masking stop. The resulting real image produced by the down-converted sideband beam is picked up by a vidicon tube and displayed on a TV monitor. The available image intensity in our setup was quite low and the TV system, with the flexibility it provides in terms of brightness and contrast, was very helpful in making the resolution observations reported below.

Figure 2 illustrates the three-dimensional nature of the system for imaging a horizontal line object. Sound from the transducer is depicted by the three arrows at the bottom of the midregion. Rays at two typical scattering points at arbitrary positions along a wire (the object) are shown. Monochromatic light arrives at the left and is formed into a cylindrically convergent beam (wedge) focused onto the z axis. Light is diffracted out of this beam wherever the sound and the light components meet the Bragg condition. The diffracted light converges to a focus that is generally quite distant from the cell.

For wires that are oriented vertically, the sound is scattered into directions with large horizontal components. This will diffract light through a focus in general much closer to the z axis than in the case of the horizontal wire orientation.

Formation of a single two-dimensional image of good quality having both horizontal and vertical line elements is possible by using an additional cylindrical lens (not shown in Fig. 2). This additional lens has the function of bringing the images for the horizontally oriented line elements to focus in the same image plane as that for the vertically oriented line elements while maintaining equal over-all magnification in both directions. (This lens is labeled horizontally oriented

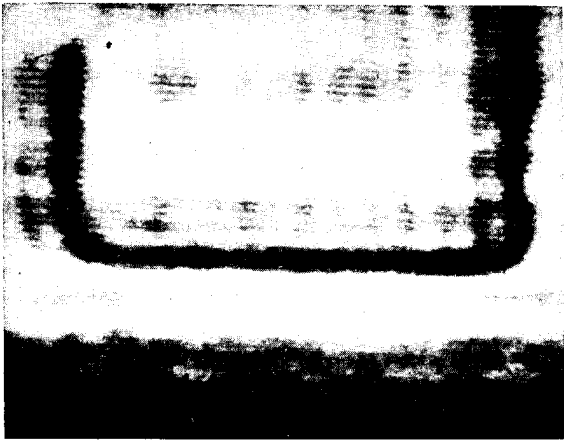


FIG. 3. Image of copper wire bent into the form of a hook with right angle bends. The wire was about 2 cm from the central plane of the light wedge. Sound wavelength was 88μ in distilled water.

cylindrical lens in Fig. 1.) Figure 3 shows a typical image obtained using for the object a 1-mm-diam wire with two right-angle bends. The vertical segment on the left was 1 cm in height. The horizontal segment was 2 cm in length. Note that the photographed size ratio of the respective segments is roughly 2 to 1, as it should be. This photograph was made by using a sound wavelength of 88μ .

II. THEORY

The test objects to be considered are either vertically oriented or horizontally oriented wires lying in a plane parallel to the y - z plane of Fig. 2. Let $U(y_0, z_0)$ be the amplitude-distribution junction for the sound pattern in the object plane. y_0 and z_0 are the y and z coordinates (Fig. 2) of an arbitrary point in the object plane. $U(y_0, z_0)$ can be expressed as a distribution of plane-wave components as calculated by means of a two-dimensional Fourier transform. The amplitude-distribution function at position y_0, z_0 can then be written

$$U(x_0, y_0) = \int_{-\infty}^{\infty} \int_{-\infty}^{\infty} U'(f, g) \exp[-j2\pi(fz_0 + gy_0)] df dg, \tag{1}$$

where f is the z_0 -directed spatial frequency and g is the y_0 -directed spatial frequency. Determination of $U'(f, g)$ follows from the Fourier transform

$$U'(f, g) = \int_{-\infty}^{\infty} \int_{-\infty}^{\infty} U(x_0, y_0) \exp[j2\pi(fz_0 + gy_0)] dz_0 dy_0.$$

Transformation to the frequency domain is consistent with a ray-tracing approach when rays are defined as a representation of differential packets (df) of plane waves. Figure 4 shows the imaging ray geometry for

the case of a horizontally oriented wire. The line extending from the position marked laser light (cb) represents a ray in the illuminating light. The indicated ray is parallel to the x - y , or horizontal, plane and is convergent to the z axis. This ray is incident at an angle α with respect to the y - z plane. The line extending from the position marked a represents a scattered sound ray in the direction of the propagation constant \mathbf{K} and wavelength Λ . This sound ray is directed at an elevation angle θ above the x - y plane. For any given sound ray, with propagation constant \mathbf{K} , there must be one light ray, with propagation constant \mathbf{k} , that satisfies the Bragg condition. This is shown at point b in Fig. 4. The diffracted ray is indicated as terminating at the location marked diffracted light, point d . The Bragg condition is satisfied when the angle between the sound and light rays is equal to the complement of the Bragg angle. The Bragg angle is given by

$$\Phi_B = \sin^{-1}[\lambda/(2\Lambda)].$$

Each sound ray produces a particular diffracted light ray that is determined by the orientation and position of that sound ray.

In Fig. 4, segment \overline{ab} is defined as a sound ray (originating at the sound source) such that light ray \overline{cb} makes the complement of the Bragg angle with respect to \overline{ab} . The resulting diffracted ray is shown as segment \overline{bd} . Point d is defined as the intersection of the diffracted ray with the x - y plane. The nature of Bragg diffraction requires that rays \overline{cb} , \overline{ab} , and \overline{bd} be necessarily in the same plane. A line parallel to ray \overline{cb} but passing through point d will lie in the x - y plane (since \overline{cb} is parallel to the x - y plane). This line intersects the ray \mathbf{K} at point a . To see this, note that d and a are, by definition, in both plane ac - bd and the x - y plane. Points a and d must then lie along the intersection of these planes.

Construct line \overline{ad} and note that angle adb equals $2\Phi_B$. It then follows that angle bad is just $\pi/2 - \Phi_B$. Triangle abd is therefore isosceles and

$$\overline{bd} = \overline{ab}/2 \sin \Phi_B = \overline{ab}(\Lambda/\lambda) = \overline{ad}.$$

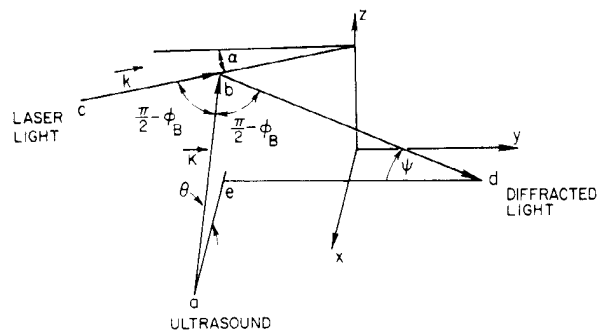


FIG. 4. Ray geometry for the light and sound interaction.

Define ψ as the angle which diffracted ray \overline{bd} makes with the x - y plane. We can then write

$$\overline{bd} \sin\psi = \overline{ab}(\Lambda/\lambda) \sin\psi = \overline{ab} \sin\theta.$$

Therefore,

$$\sin\theta/\Lambda = \sin\psi/\lambda. \quad (2)$$

The left side of Eq. 2 is a z -directed spatial frequency in the sound field. The right side is a z -directed spatial frequency in the diffracted light field. Equation 2 states that the z -directed spatial frequencies (f_{zi}) in diffracted light will reproduce the z -directed spatial frequencies (f_{zs}) in the scattered sound field. (Note that f_{zs} is the same spatial frequency as f in Eq. 1.)

Before determining a similar relation for the y -directed spatial frequencies, let us generalize to some extent by permitting the scattered sound to have an azimuthal component (i.e., a component in the y direction). Under these circumstances we make the following observation. A sound ray at any given elevation angle θ and azimuthal angle β_s (measured in the x - y plane) will uniquely define the orientation of the resulting diffracted ray. This fact is a direct consequence of the selection property of diffraction due to sound. Therefore, if incident light rays exist for all possible values of α , rotation of the sound cell about the z axis by an angle β_s (which thereby rotates the sound source and scattering object) will simply produce a corresponding azimuthal rotation (i.e., a rotation about the z axis) of diffracted light rays. Let Δ be the angle of rotation of the diffracted light rays. Then, as we have just stated,

$$\Delta = \beta_s. \quad (3)$$

Note that Eq. 3 is a general equation which holds regardless of how the azimuthal angle for the sound (β_s) is produced. The equation does not depend upon rotating the sound cell for its validity. Any sound ray having an azimuthal angle β_s for whatever reason can be regarded as having been rotated through the angle β_s . The related diffracted light ray can then also be regarded as having been rotated through the same angle, in accordance with Eq. 3. Thus we can use Eq. 3 to relate any sound ray at azimuthal angle β_s (and elevation angle θ) to the resulting diffracted light ray.

We can simplify the analysis by defining a new coordinate system x', y', z' . Let e of Fig. 4 be a point directly below point b . The origin of the new system is at point e . The x' axis lies within the x - y plane and points in the direction of the horizontal projection onto the x - y plane of the sound ray being considered. The z' axis points in the vertical direction and therefore passes through b . The new system is illustrated in Fig. 5.

By applying the law of cosines to triangle aod and using Eq. 2, we obtain

$$\cos\left(\frac{\pi}{2} - \gamma\right) = \left(\frac{\lambda}{2\Lambda}\right) \frac{(\cos^2\theta - \sin^2\theta)}{\cos\theta\{1 - [(\Lambda/\lambda)\sin\theta]^2\}^{\frac{1}{2}}}, \quad (4)$$

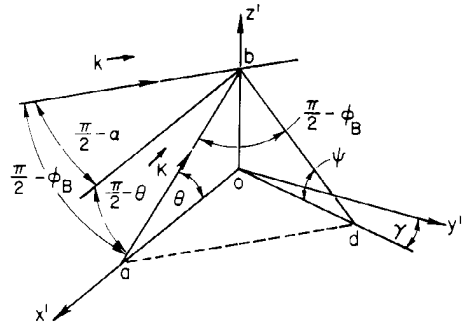


FIG. 5. Ray geometry in terms of the new coordinate system x', y', z' . Note that the origin o coincides with the point e of Fig. 4.

where the angle γ is $\pi/2$ minus the angle aod and is illustrated in Fig. 5. The experimental work reported here concerns sound wavelengths at least 100 times the light wavelength. To good approximation, then, Eq. 4 can be written

$$\sin\gamma \cong (\lambda/2\Lambda) \cos 2\theta / \cos\theta. \quad (5)$$

If we eliminate rays with elevation angles greater than 88° , the magnitude of $\sin\gamma$ will not be greater than about 0.14 if the ratio of wavelengths (Λ/λ) is at least 100. We can then use a small-angle approximation for $\sin\gamma$. The azimuthal direction of the diffracted light ray is a function of the z -directed spatial frequency of that light ray since θ is a function of f_{zs} and hence of f_{zi} . The azimuthal angular direction with respect to the y axis of the diffracted ray for a sound ray with arbitrary azimuthal direction is then approximately

$$\gamma - \Delta \cong (\lambda/2\Lambda) \cos 2\theta / \cos\theta - \beta_s \quad (\theta < 88^\circ). \quad (6)$$

If β_s is limited to fairly small values, we can write

$$f_{xi} \cong (1/2\Lambda) \cos 2\theta / \cos\theta - (\Lambda/\lambda) f_{ys} / \cos\theta. \quad (7)$$

Note that f_{ys} is the same spatial frequency as g in Eq. 1. Equations 2 and 7 state that spatial frequencies in the diffracted light field are simply related to spatial frequencies describing scattered sound. Note that in Eq. 7, f_{xi} differs from f_{ys} by a quantity dependent upon θ . This is related to the aberrations referred to in the introduction.

Now consider a long wire with vertical orientation. Such a wire will scatter sound radially with almost no vertical components. Small-angle approximations were previously used to obtain the simple relation expressed by Eq. 7. However, if θ is small, we may get a relation without any approximation. To get such a relation, define a line x'' in the x - y plane of Fig. 4 where x'' makes an angle Φ_B with respect to the x axis. For spatial frequencies defined in terms of the direction of this line, we can write

$$f_{x''i} = \sin\Delta/\lambda = (\Lambda/\lambda) f_{ys}. \quad (8)$$

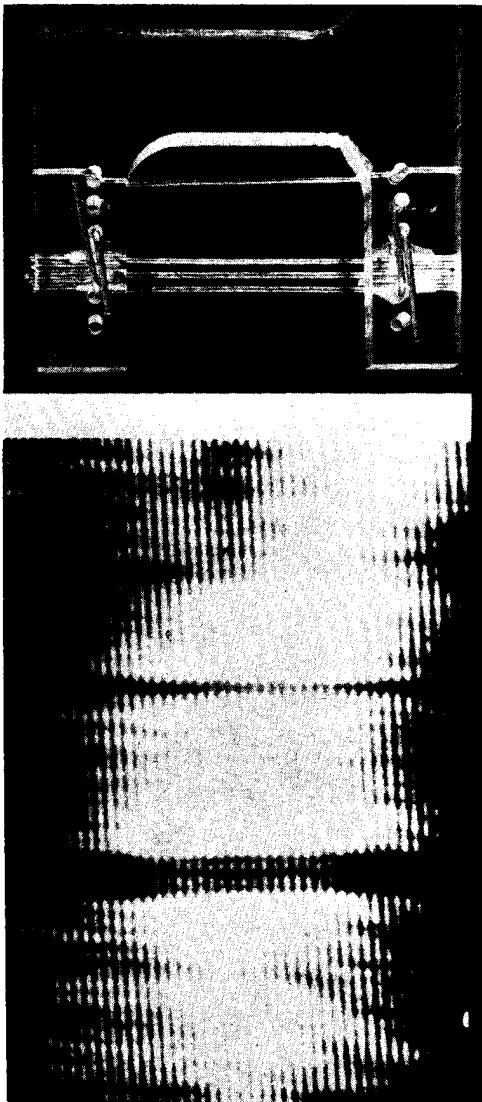


FIG. 6. Test object consisting of small parallel wires (upper figure) and typical image of test object (lower figure). Image on the bottom was made with copper wires 125μ in diameter. The maximum θ was 20° and the sound wavelength was 88μ .

Consider a vertical observation screen for imaging the vertical line. The screen is oriented parallel to the x'' line. Equation 8 states that the horizontally directed spatial frequency on this screen is proportional to y -directed spatial frequencies in the sound field. Note that Eq. 8 is the simple relation we seek, and it holds as long as z -directed spatial frequencies are absent.

The proportionality factor Δ/λ in Eqs. 7 and 8 indicates the need for magnification by Δ/λ in the horizontal direction to obtain an image with the correct aspect ratio.

If a wire oriented in the y direction is of uniform cross section, f_{ys} will be on the order of, or less than, the reciprocal of the length dimension (for all rays of significance). Only the first term on the right side of

Eq. 7 will be of significance. In that case, rays of high z -directed frequencies will arrive offset from rays with low z -directed frequencies. This ray offset is properly described as an aberration. However, the effect of this aberration is small when the object viewed is a long wire oriented horizontally. Equation 8 has no aberration term and therefore shows that aberrations are not important to the formation of an image of a wire oriented vertically. We therefore conclude that test objects consisting of vertical or horizontal wires can be imaged without significant aberration effects.

Our experiments were concerned with the resolution of three copper wires of equal diameter with the spacing between the wires equal to the diameter. The form of the object used is illustrated in Fig. 6. Wires of various sizes were mounted as shown on the fixture at the top. When the wires were near the resolution limit in size, the observed image looked similar to the photograph at the bottom of Fig. 6. The lower photograph was made using horizontal wires that were 125μ in diameter and about 1 cm in length. A sound wavelength of 88μ (in water) was used. The interaction aperture was limited by the height of the illuminating light wedge. When this picture was taken, the maximum possible θ was equal to 20° .

To facilitate the theoretical analysis we considered the arrangement of parallel wires as simply alternate opaque and transparent bands (or slits). Analysis of this simplified model follows by taking the Fourier transform of an amplitude distribution like that shown in Fig. 7. The result is completely analogous to a frequency spectrum of temporal pulses. We therefore turn to a well-known result concerning passband requirements to resolve rectangular pulses. Goldman⁶ shows that two pulses of equal length and equal spacing can be resolved if the highest passband frequency is the reciprocal of twice the length of one pulse. In this case, resolution is indicated by two amplitude peaks separated in a valley that is about 25% of peak value. It is well known that any number of pulses can be easily distinguished in the noise-free case if the receiver passband is at least equal to

$$f = 1/2D,$$

where D is the pulse length.

Note that the application of the above analytical result to our system implies that we are illuminating

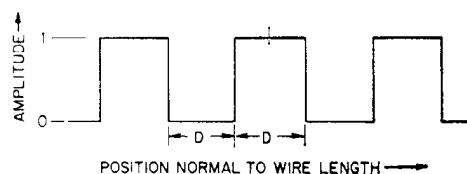


FIG. 7. Waveform simulation of objects used in the resolution experiments.

an object with a transmission function of the form shown in Fig. 7 with coherent sound. Thus we expect to easily resolve wires of diameter D if the system delivers spatial frequencies up to

$$f - \sin\phi_m/\lambda - 1/2D,$$

where $\sin\phi_m$ is the numerical aperture. Resolution of the system will then be expressed by

$$D = \lambda/2 \sin\phi_m. \quad (9)$$

Long thin fibers of thickness and separation equal to D_{ih} should then be resolved at the image plane when oriented horizontally if (from Eq. 9)

$$D_{ih} = \lambda/2 \sin\psi_m, \quad (10)$$

where ψ_m is the maximum elevation angle that the diffracted light rays can have and the subscripts *ih* stand for image horizontal.

The maximum possible value of the angle θ of Fig. 4 is often limited by the height of the illuminating wedge of light. Determination of θ_m follows from simple geometrical considerations. θ_m is then given by the half-angle subtending the wedge. It is easy to achieve a θ_m as large as 88° if the object is at the light wedge edge.

In terms of object plane variables Eq. 10 becomes (using Eq. 2)

$$D_{oh} = \Lambda/2 \sin\theta_m, \quad (11)$$

where the subscripts "oh" stand for object horizontal.

Resolution of vertical wires is limited by the angular width of the light wedge. Let α_m be the angular portion of the wedge from which the down-converted image is constructed. Then from Eq. 9 we have

$$D_{iv} = \lambda/2 \sin\alpha_m, \quad (12)$$

where the subscripts "iv" stand for image vertical. An image the same size as the object is obtained only when the horizontal detail is magnified by the ratio Λ/λ .³ In terms of the object plane variables the above equation becomes

$$D_{ov} = (\Lambda/\lambda)D_{iv} = \Lambda/2 \sin\alpha_m, \quad (13)$$

where the subscripts "ov" refer to "object vertical."

Note that Eqs. 11 and 13 are of the same form as the Rayleigh expression for line sources with axis separation equal to D_{ov} or D_{oh} , as applicable.

III. EXPERIMENTAL RESULTS

Experimental verification of the case with the wire axis oriented vertically was attempted using a light wedge corresponding to $\sin\alpha_m = 1/10$. We would then expect (from Eq. 13) to be able to resolve wires as small as five sound wavelengths in diameter. However, wires arranged as in Fig. 6 with diameters equal to 10 sound wavelengths could barely be resolved under these conditions.

Experimental verification of the case with the wire axis oriented horizontally was attempted over a wide range of conditions. The distance between an object (like that in Fig. 6) and the light wedge was varied. The height (z direction) of the wedge was also varied. Evaluation of the results for each case where θ_m was about 40° or less gave results in good agreement with Eq. 11. It was possible to obtain values of θ_m nearly as large as 90° by placing the object wires very close to the light wedge. We would then expect to resolve wires as small as one-half wavelength. The resolution was almost that good. Copper wires of diameter as small as two-thirds of a sound wavelength could barely be resolved.

IV. DISCUSSION

Resolution in the present context is subjective since it depends upon a human observer. The observer usually knows what he is supposed to see. Typically (and certainly here) it is only a question of deciding whether there are one, two, or three (or more) like elements of known form in an image. Noise and other patterns unrelated to the test object will influence observations that in these experiments were attempts at determining the minimum conditions under which something can barely be seen. Differences between theory and experimental results are therefore expected.

The ray-path diagrams that were initially constructed showed that aberrations are intrinsic to the Bragg imaging system for horizontal wires. However, the resolution analysis indicated that we could neglect the effect of these aberrations. No aberrations exist for vertical wires.

The resolution of our experimental system is of quite different character for vertical wires than for horizontal wires. It should be possible to design a system with equal resolution in both directions. Equations 11 and 13 show that this requires a wedge angle equal to the vertical angle subtending the wedge height as seen at the object. However, it will always be easier to achieve high resolution for horizontal wires than for vertical wires. This is because diffracted light rays must be brought to focus from a much wider angle for the horizontal wires than for the vertical wires if the resolution is to be equal.

V. CONCLUSION

In this paper we have analyzed and measured the resolution obtainable with a Bragg imaging system. Study of ray-path diagrams initially led us to the conclusion that the best objects for experimentation would be long cylinders oriented either vertically or horizontally. These types of objects minimize the effects of aberrations that are inherent in the system. This conclusion is predicted by the analysis and is borne out by the experiment.

Analysis showed that the spatial frequency spectrum of the scattered sound would generally be reproduced with good fidelity in the diffracted light. Expressions for the theoretical resolution for each orientation of the wires (Eqs. 11 and 13) were derived by finding the maximum spatial frequencies that could be passed by the system. Experimental results agreed reasonably well with the predicted values. For vertical wires the experimentally obtained minimum resolvable diameter was 10λ and for horizontal wires, $\frac{2}{3}\lambda$.

ACKNOWLEDGMENTS

The research for this paper was sponsored in part by a grant from the National Institutes of Health. The

authors express appreciation to Professor Glenn Heidbreder of the University of California, Santa Barbara, for reading and commenting on the manuscript.

* Present address: Dept. of Elec. Eng., Sacramento State College, 6000 J St., Sacramento, Calif. 95825.

¹ L. Brillouin, *Ann. Phys. (Paris)* **17**, Ser. 9, 88-122 (1922).

² M. G. Cohen and E. I. Gordon, *Bell System Tech. J.* **44**, 693 (1965).

³ A. Korpel, *Appl. Phys. Lett.* **9**, 425-427 (1966).

⁴ J. Landry, J. Powers, and G. Wade, *Appl. Phys. Lett.* **15**, 186-188 (1969).

⁵ A. Korpel, private communication (1969).

⁶ S. Goldman, *Frequency Analysis, Modulation and Noise* (McGraw-Hill, New York, 1948), 1st ed., pp. 84-85.